HYDROGEN STORAGE PROPERTIES OF MAGNESIUM BASE NANOSTRUCTURED COMPOSITE MATERIALS

Ming Au*

Savannah River Technology Center
Aiken, SC 29803

Key words: Magnesium, hydrogen storage, nanostructured materials, composite

ABSTRACT

In this work, nanostructured composite materials Mg-Ni, Mg-Ni-La, Mg-Ni-Ce and Mg-$LaNi_5$ have been synthesized using the mechanical alloying process. The new materials produced have been investigated by X-ray diffraction (XRD), transition electron microscope (TEM), scanning electron microscope (SEM) and electron energy dispersion spectrum (EDS) for their phase compositions, crystal structure, grain size, particle morphology and the distribution of catalyst element. Hydrogen storage capacities and the hydriding-dehydriding kinetics of the new materials have been measured at different temperatures using a Sieverts apparatus. The results show that amorphous/nanostructured composite material Mg50%-Ni50% absorbs 5.89wt% within five minutes and desorbs 4.46% hydrogen within 50 minutes at 250^{o}C respectively. Adding 5% La into Mg-Ni composite materials reduces the starting temperature of hydrogen absorption and desorption from 200^{o}C to 25^{o}C which suggests the formation of unstable hydrides. The composite material Mg80%-$LaNi_5$ 20% absorbs 1.96% hydrogen and releases 1.75 wt% hydrogen at 25^{o}C. It is observed that mechanical alloying accelerates the hydrogenation kinetics of the magnesium based materials at low temperature, but a high temperature must be provided to release the absorbed hydrogen from the hydrided magnesium based materials. It is believed that the dehydriding temperature is largely controlled by the

thermodynamic configuration of magnesium hydride. Doping Mg-Ni nano/amorphous composite materials with lanthanum reduces the hydriding and dehydriding temperature. Although the stability of MgH_2 can not be easily reduced by ball milling alone, the results suggest the thermodynamic properties of Mg-Ni nano/amorphous composite materials can be alternated by additives such as La or other effective elements. Further investigation toward understanding the mechanism of additives will be rewarded.

1. Introduction

Magnesium and its derived alloys are looked upon as promising candidates of hydrogen storage due to their high theoretical storage capacity (7.6 wt%), light weight and low cost. However, high operating temperatures and slow kinetics prevent them from practical application [1-2]. Multi-component Mg base alloys have met with limited success in increasing kinetic dynamics and lowering the desorption temperatures [3-6]. Efforts to seek new ternary Mg hydrides with favored reaction kinetics and temperature have not produced promising results [7-9]. A number of reports show that the reaction kinetics have been accelerated significantly, even at ambient temperature using nanostrucutred or amorphous Mg based materials synthesized by ball milling or mechanical alloying [10-12]. Unfortunately, the desorption temperature of the studied Mg based materials was still too high to be used practically. In most cases, it required at least 250^oC to liberate hydrogen from magnesium hydrides. To explore the possibility and

assess the reality of lower desoprtion temperatures, several amorphous/nanostructured composite Mg based materials have been investigated. The results are presented in this paper.

2. Experimental

Stoichiometric and non-stoichiometric Mg based materials were synthesized by a mechanical alloying process. Pure metal powder Mg, Ni, La, Ce and Zr were purchased from Alfa Aesar and Cerac. The purity and particle size are 99.5% and 100 μm respectively. Five grams of precursor powder was weighed and mixed with two tungsten carbide balls (ϕ7/16") in an airtight tungsten carbide jar. The jar was loaded in a SPEX-8000™ high-energy ball mill and shaken for a selected periods of time. Every two hours, the jar was taken into a glove box for removal of the material adhering on the wall. The average grain size was reduced gradually by the ball milling, see Fig.1. In this work, the mechanical alloying process took about 50-60 hours for synthesis of amorphous materials and 20-30 hours for preparation of nano/amprphous composite materials. To avoid any possible oxidation, the powder was handled and processed in an argon-filled glove box.

The crystal structures, phase compositions and grain size of the new materials were investigated using a Philips™ X-ray diffractometer. The morphology, fine crystalline features and element distributions were observed using Hitachi 8100S™ TEM and JEOL JSM-5800™ SEM. The kinetics of hydrogen absorption and desorption of new materials were measured using a manual controlled Sieverts apparatus equipped with computer

data acquisition. The hydrogen absorption was conducted at 3 MPa and the hydrogen desorption was conducted at vacuum and at different temperatures. The pressure-composition-isotherms (PCI) were measured by an automatic Sieverts volumetric analysis instrument at a commercial service laboratory.

3. Results and discussion

3.1 Mg 50wt% - Ni 50wt % amorphous materials

XRD indicates the three grams of Mg 50wt% - Ni 50wt % powder mixture was transformed to amorphous materials after ball-milling for 50 hours (Fig.1). TEM observation found no crystalline structure existed in the new material (Fig.2). This amorphous material started to absorb hydrogen at 200^{o}C rapidly (Fig.3). The material absorbed 1.8 wt% hydrogen within the first three minutes and 1.9 wt% within first five minutes at 250^{o}C. However, desorption was incomplete at the same temperature. Only 1.3 wt% hydrogen was desorbed at 250^{o}C (Fig.4). About 0.6 wt% hydrogen still remaining in the material desorbed at 300^{o}C. Increasing the temperature helps hydrogen desorption because of its endothermic nature. But, the high temperature is not always favorable for the exothermic hydrogen absorption. There is an optimal temperature for hydrogen absorption. With our experimental condition, the 250^{o}C was the best temperature for hydrogen absorption (Fig.3). This is consistent with our early work on magnesium materials [13,14].

3.2 Mg 50wt% - Ni 50wt % amorphous/nanostructured composite materials

Three grams of Mg 50 wt% - Ni 50wt % powder mixture was ball-milled for only 30 hours. XRD indicates that the new material synthesized by the 30 hour ball milling is a composite that consists of nanostructured magnesium and amorphous nickel (Fig.5). The average grain size of magnesium was reduced gradually with increase of milling time. The trend of the grain size reduction slows down approaching a limit. From the peaks of Mg in the XRD spectrum, the average grain size of Mg after 30 hour of milling is calculated as 13 nm (Fig. 6). The TEM shows that the nanocrystalline Mg grains are surrounded by amorphous Ni inter-grain regions (Fig.7). The nanocrystalline structure of magnesium matrix and the amorphous state of nickel inter-grain regions are identified by localized electron diffraction (Fig.8-9). The Mg 50wt% - Ni 50wt % amorphous/nanostructured composite material was tested at 200^{o}C, 250^{o}C and 300^{o}C for its hydrogen absorption and desorption properties. Although no hydrogen absorption was observed under 200^{o}C, the material surprisingly absorbed 6.9 wt% hydrogen at 250^{o}C (Fig.10). The kinetics of hydrogenation was impressively fast. At 250^{o}C, the material absorbed 95% of its hydrogen capacity within the first three minutes. The hydride decomposed and released 4.5 wt% hydrogen at 250^{o}C (Fig.11). As pointed out above, the hydrogen desorption was slower than absorption. At 250^{o}C, it took 60 minutes to release 4.5 wt% hydrogen. It was determined that about 2.4 wt% hydrogen still remained in the material at 250^{o}C. By raising the temperature to 300^{o}C, the hydrogen desorption was increased to 5.5 wt% at an acceptable rate (Fig.11).

It was found that the hydrogen storage capacity of the nano-amorphous composite material was much higher (6.9 wt%) than its amorphous counterpart (1.9 wt%) by comparing the two materials with the same chemical composition. It is believed that the inherent structure disorder in amorphous alloys places additional restrictions on the number of interstitial sites that are favorable for hydrogen to occupy [15]. A model of the nano/amorphous composite structure illustrates its advantage in regards to hydrogen storage properties (Fig.12). In amorphous material, the magnesium and nickel atoms are arranged randomly with no order. There are no favorable interstitial sites for hydrogen atoms to occupy. This causes low hydrogen storage capacity. Furthermore, the disordered structure does not have the channels such as grain boundaries and interfaces for rapid hydrogen diffusion. This results in the slow reaction kinetics. However, in the nanostructured-amorphous composite material, the nanocrystalline magnesium structure provides a great number of interstitial sites and fine grain boundaries that favors hydrogen migration and residence resulting in a high storage capacity. Meanwhile, the amorphous nickel clusters surrounding nanostructured magnesium play the role of catalysts, spliting the molecular hydrogen into atoms. The hydrogen atoms diffuse and penetrate into the area along the interface between the amorphous and nanostructure phases, resulting in the fast hydrogenation kinetics.

3.3 Pressure-Composition-Isotherms (PCI) of the amorphous/nanostrctured composite Mg50wt%+Ni50wt% material

The thermodynamic properties of the amorphous/nanostructured Mg50% -Ni50% composite material were measured in an automatic Sievert device. The Pressure-

Composition-Isotherms (PCI) of hydrogen desorption at different temperatures are shown in Fig.13. The hydrogen storage capacities were confirmed as 1.65 H/M (6.9 wt%) at 300^{o}C. The equilibrium pressure at 300^{o}C was 12 psia. This high capacity is close to its theoretical value of MgH_2. It is believed that the amorphous/nanostructured Mg50% - Ni50% composite material is the ideal candidate for hydrogen storage with the high capacity if its hydrogen desorption temperature can be reduced to a reasonable level by modifying its thermodynamic stability. Two plateaus were observed in the 300^{o}C isotherm that imputes two hydrides formed during hydrogenation. One is less stable (some type of Mg-Ni-H hydride) than the another (MgH_2). There is an interruption in the PCI at 250^{o}C due to the very low equilibrium pressure and the limits of vacuum system on the instrument. For the same reason, the PCI at 200^{o}C was not able to be measured.

3.4 Mg-Ni-La nanocrystalline/amorphous composite materials

Three Mg-Ni-La nano/amorphous composite materials, Mg60%-Ni30%-La10%, Mg70%-Ni20%-La10% and Mg80%-Ni15%-La5% were synthesized by 24 hour ball milling. The investigation on their hydrogen storage properties found that La addition (1) reduced the hydrogen absorption temperature from 200^{o}C to room temperature compared with Mg50%-Ni50% composite material; (2) reduced the starting temperature of hydrogen desorption from 200^{o}C to 25^{o}C; (3) increased the hydriding and dehydriding rates; and (4) reduced the hydrogen storage capacity (Fig. 14-19). It was determined that adding lanthanum changes the stability of magnesium hydrides, improves the kinetics and reduces the hydrogen storage capacity. It is believed that there is an optimal percentage of lanthanum for fast discharge rates and sufficient hydrogen storage capacity. The

mechanism of lanthanum's role is not yet clearly understood. One possible explanation is that there may be some new intermetallic Mg-La-Ni compounds formed during ball milling resulting in less stable thermodynamics of their hydrides. The large jump in hydrogen absorption from 200^{o}C to 300^{o}C raises our attention. At 300oC, the hydrogen absorption behavior appears to be dominated by magnesium. But, under 200^{o}C, the hydrogen absorption may be attributed to Mg-La compounds such as La_2Mg_{17}. Its hydrogen absorption properties (1.7wt% and 5.5 wt%) at low temperature have been reported by Darriet (1.7 wt%) [16], Dutta (6.05wt% at 25^{o}C) [17] and Yajima (1.7wt% at 100^{o}C) [18]. Further investigation is needed.

3.5 Mg-Ni-Ce nanocrystalline/amorphous composite materials

The materials, Mg60%-Ni30%-Ce10% and Mg70%-Ni20%-Ce10% were synthesized by 24 hour ball milling. The evaluations of their hydrogen storage performance is shown (Fig. 20-21) Ce was found to be less efficient than La in improving hydrogen capacity. For example, Mg70%-Ni20%-La10% absorbed 1.6 wt% hydrogen at 25^{o}C, but Mg70%-Ni20%-Ce10% absorbed only 0.7 wt% hydrogen at the same temperature. The hydrogen storage capacity of Mg-Ni-Ce system is significant lower than the Mg-Ni-La system. For example, Mg60%-Ni30%-Ce10% absorbed 3.8 wt% hydrogen at 300^{o}C, but Mg60%-Ni30%-La10% absorbed 6.1 wt% hydrogen at the same temperature. The different configuration of the valence electrons of Ce ($4f^2 6s^2$) than La ($5d^6 s^2$) may contribute to this negative effect. Therefore, the Mg-Ni-Ce system is not worthy of further investigation.

3.6 Mg-$LaNi_5$ system

The Mg-$LaNi_5$ system has the potential to be developed as a rapid discharge hydrogen storage material at ambient temperatures. $LaNi_5$ is appreciated for its fast hydriding and dehydriding kinetics at ambient temperature, but its storage capacity is low. Mg is known for its high capacity among known metal hydrides, but its hydrogen desorption rate is too slow, even at high temperature (300^{o}C). The goal is to develop a Mg-$LaNi_5$ system that combines the advantages of the both materials. In this work, three Mg-$LaNi_5$ composite materials, Mg80%-$LaNi_5$20%, Mg75%-$LaNi_5$25% and Mg60%-$LaNi_5$40%, were synthesized by 30 hours of ball milling. The results of hydrogen storage measurement of the Mg-$LaNi_5$ system are shown in Fig.22-27. It was found that the addition of $LaNi_5$ reduced the starting temperature of hydrogen absorption; led to excellent kinetics at room temperature and yield high hydrogen storage capacity at elevated temperatures. It was also found that hydrogen storage capacity decreased with increasing $LaNi_5$ ratio. For example, the starting temperature of hydrogen absorption of Mg80%-$LaNi_5$20% was reduced to 25^{o}C. Mg80%-$LaNi_5$20% absorbed and desorbed 1.9 wt% and 1.7 wt% hydrogen respectively at room temperature within two minutes. Mg80%-$LaNi_5$20% desorbed 1.9 wt% and 5.1 wt% hydrogen at 200^{o}C and 300^{o}C respectively. The capacity decreased from 6.5 wt% for Mg80%-$LaNi_5$20% to 3.5 wt% for Mg60%-$LaNi_5$40% at 300^{o}C. As seen, there is a large jump inthe hydrogen absorption and desorption capacity from 200^{o}C to 300^{o}C. This implies that the material behavior is dominated by $LaNi_5$ at

low temperature and by Mg at high temperature. As XRD shows in Fig. 29, there are still two phases, nano-crystalline $LaNi_5$ and nano/amorphous Mg, in Mg85%-$LaNi_5$20% powder after 60-hours ball milling. The EDX mapping of Mg, Ni, and La indicates that the distributions of Ni and La do not always reflect the formula of $LaNi_5$. At certain level, the separation of Ni with La is expected during ball milling (Fig.29).

These experimental results indicated to us an opportunity that the room temperature capacity may be increased further if the $LaNi_5$ phase is distributed homogeneously on the magnesium matrix. There are two ways to do this: (1) extending the milling time; and (2) annealing the powder below the recrystallization temperature to allow $LaNi_5$ to diffuse into Mg phase. The SEM images of Mg85%-$LaNi_5$15% before and after hydrogenation (10 cycles) are given by Fig.30-33. A number of tiny hydride particles form after hydrogenation. Hydrogenation also creates a great deal of cracks resulting in material pulverization. As the pictures show, the average particle size is reduced remarkably after hydrogenation.

4. Conclusion

Nano/amorphous composite materials can be synthesized by mechanical alloying. The experiment results show that with the same composition, the Mg-Ni nano/amorphous composite materials are superior to their amorphous counterparts in hydrogen storage capacity and kinetics. This may be attributed to the unique composite structure or the combination of the nanocrystalline magnesium matrix and the amorphous nickel inter-grain region. The Mg matrix provides a great number of diffusion channels and

interstitial sites for hydrogen migration and reaction. The Ni cluster network surrounding the Mg matrix can play a catalytic role during hydriding/dehydriding reaction. The Mg50%-Ni50% nano/amorphous composite material absorbed 6.9 wt% hydrogen within five minutes and desorbed 4.5 wt% hydrogen within 50 minutes at 250^{o}C. Adding $LaNi_5$ in magnesium improves the hydrogen storage performance at room temperatures. The nano/amorphous composite material Mg 80%-$LaNi_5$20% absorbed and desorbed 1.9 wt% and 1.7 wt% hydrogen at 25^{o}C respectively. By increasing the temperature, this material desorbed 1.9 wt% hydrogen at 200^{o}C and 5.1 wt% hydrogen at 300^{o}C. The nano/amorphous composite structure improved the hydriding-dehydriding kinetics, reduced hydriding temperature and enhanced hydrogen storage capacity of magnesium based materials. It is believed that the dehydriding temperature is largely controlled by the configuration of magnesium hydride. Adding lanthanum into Mg-Ni nano/amorphous composite materials reduced the hydriding and dehydriding temperature from 200^{o}C to 25^{o}C. This indicates that the thermodynamic stability of Mg-Ni nano/amorphous composite materials can be reduced by additives such as La or other effective elements. Further investigation and understanding of the mechanism is recommended.

ACKNOWLEDGEMENTS

This work has been done in Nanomaterials Research Corporation (Longmont, CO) in 1999, financially supported by NASA under contract NAS9-98089. Author thanks Drs. Ted Motyka, Ragaiy Zidan and Tom Walters of Savannah River Technology Center for their comments and suggestions on this paper.

REFERENCES

[1] J.J.Reilly and R.H.Wiswall, Inorg.Chem. 6(1967)2220

[2] B.Darriet, M.Pezal et al, Int.J.Hydrogen.Energy. N2 (1980)173

[3] J.J.Reilly and R.H.Wiswall, Inorg.Chem. 7(1968)2254

[4] A.Karty,J.Grunzwig-Genossar and P.S.Rudman, J.Appl.Phys. V50, N11(1979)7200

[5] D.L.Douglass, Met.Trans. 6A(1975)2186

[6] M. Au, J.Wu, Q-D Wang, Int.J.Hydrogen Energy, V20, N2(1995)141

[7] H.A.Aebischer and L.Schlapbach, Z.Phys.Chem. 179.S(1993)21

[8] K.Kadir and D.Noreus, Z.Ohys.Chem. 179.S(1993)243

[9] B.Huang, K.Yvon and P.Fisher, J.Alloys.Comp. 227(1995)121

[10] A. Zaluska, L.Zaluski, J.O.Strom-Olsen, J.Alloys.Comp.288(1999)217

[11] G.Liang, J.Huot, S.Boily,A.V.Neste,R.Schulz, J.Alloys Comp.292(1999)247

[12] J.Huot, J.F.Pelletier, L.B.Lurio, M.Sutton, R.Schulz, J.Alloys.Comp. 348(2003)319

[13] M. Au, J. Wu, Q.D. Wang, Hydrogen Energy Progress V, 1279-1290,

[14] M. Au, J. Wu, Q.D. Wang, Int.J.Hydrogen Energy, V20, N2(1995) 141-150

[15] R.Bowman, Materials Science Forum V31(1988)197-228

[16] B.Darriet et al, Int.J.Hydrogen Energy V5 (1980)173-178

[17] Dutta et al, Hydrogen Energy progress VIII, V2(1990)1027-1034, Pergamon Press.

[18] S.Yajima et al, J.Less-Comm.Met. V55(1977)139-141

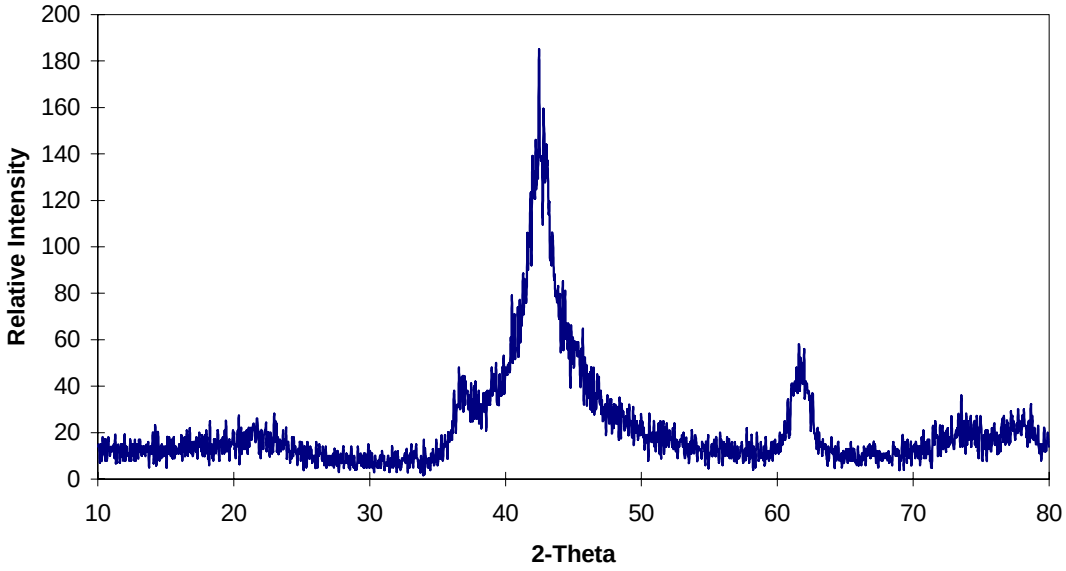

Fig.1 XRD spectrum of the materials Mg50%- Ni50% after 50 hour ball milling. The broaden peaks does not correspond to either Ni or Mg. It may be caused by high mechanical stress. The raised background suggests the material is in amorphous state in general.

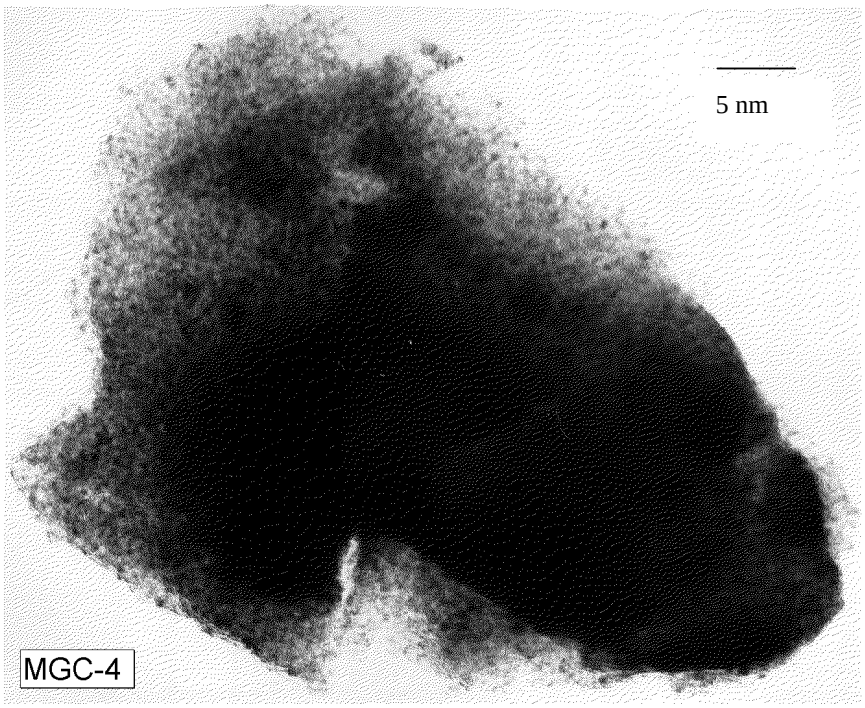

Fig. 2 TEM image of the material Mg50% - Ni50% after 50 hour ball milling. Generally, the material is in amorphous state.The heavily deformed nanocrystalline structure may exist, but not be observed.

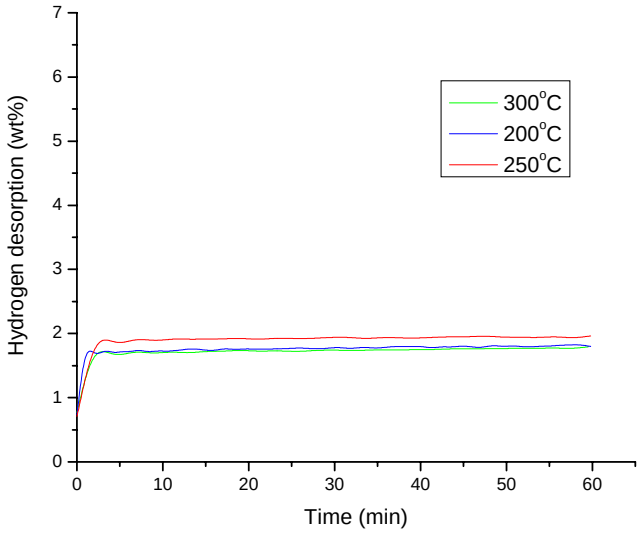

Fig. 3 Hydrogen absorption of the amorphous material Mg50%-Ni50%

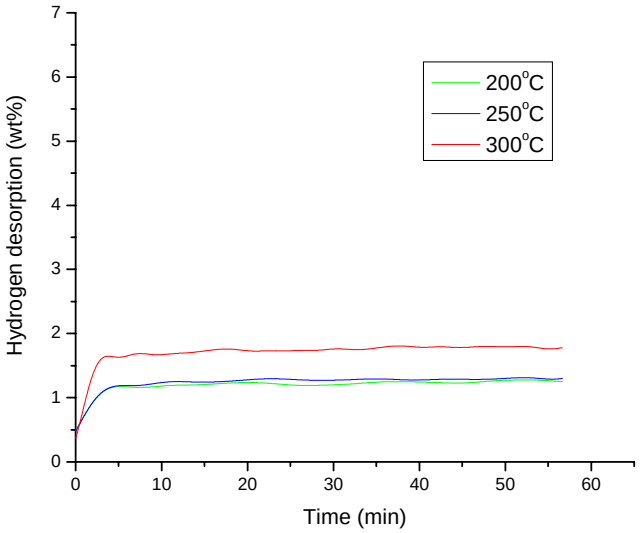

Fig. 4 Hydrogen desorption of the amorphous material Mg50%-Ni50%

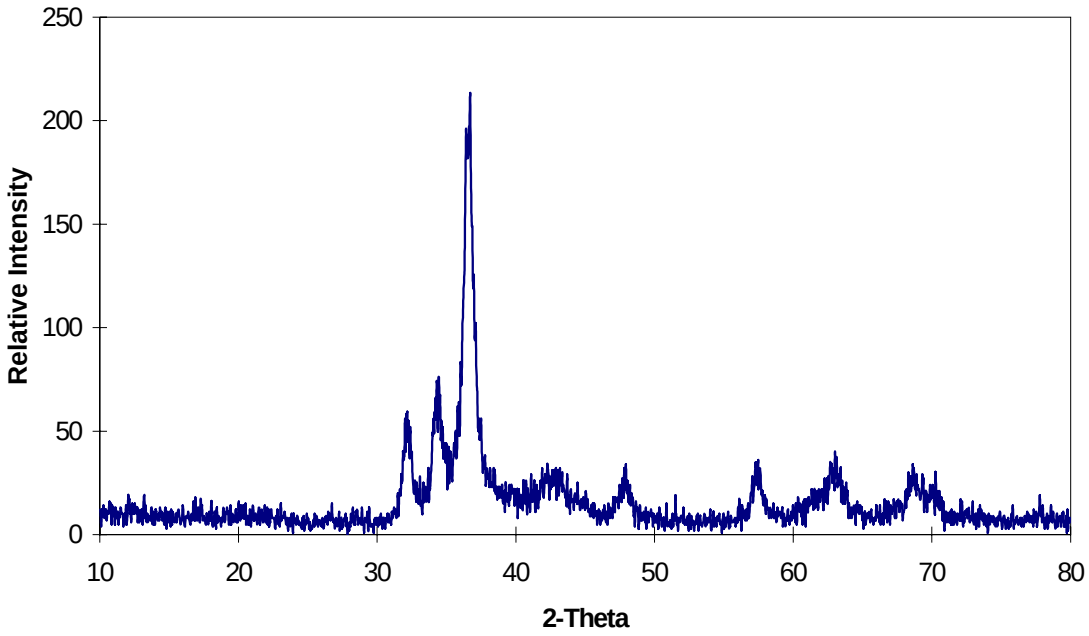

Fig. 5 XRD spectrum of the 30 hour ball milled material Mg50%+Ni50%. The broaden peaks correspond to Mg. There is no Ni peaks identified. It is believed that the material is a composite consisting of nanostructured Mg and amorphous Ni

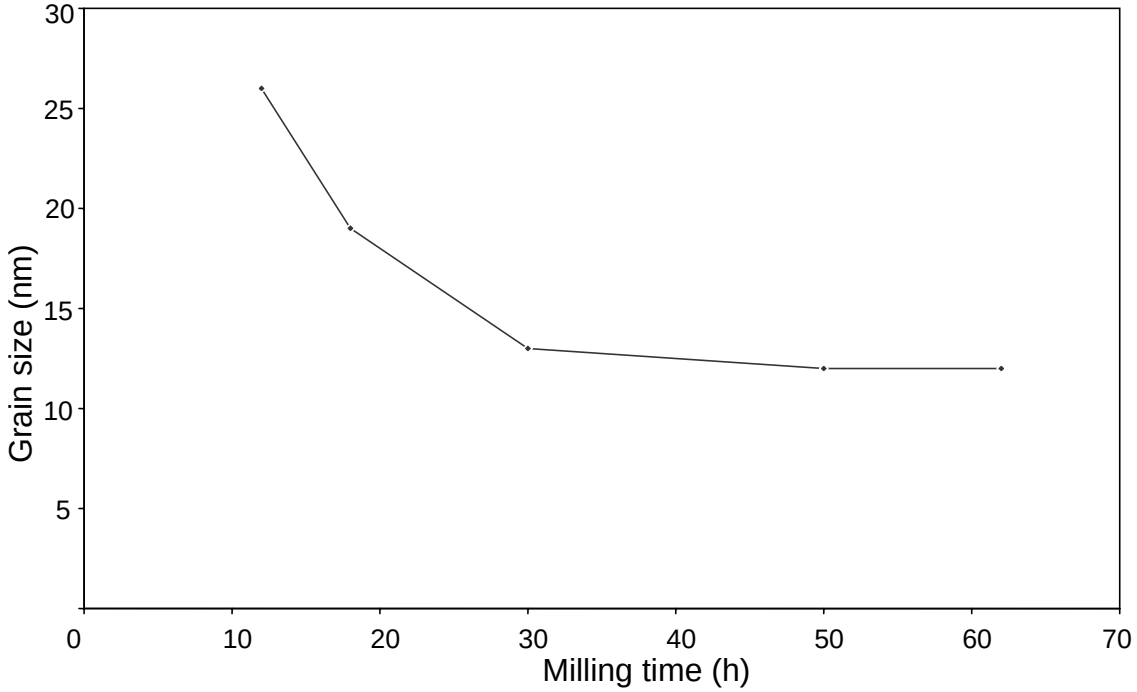

Fig.6 The average grain size of Mg-Ni materials after ball milling

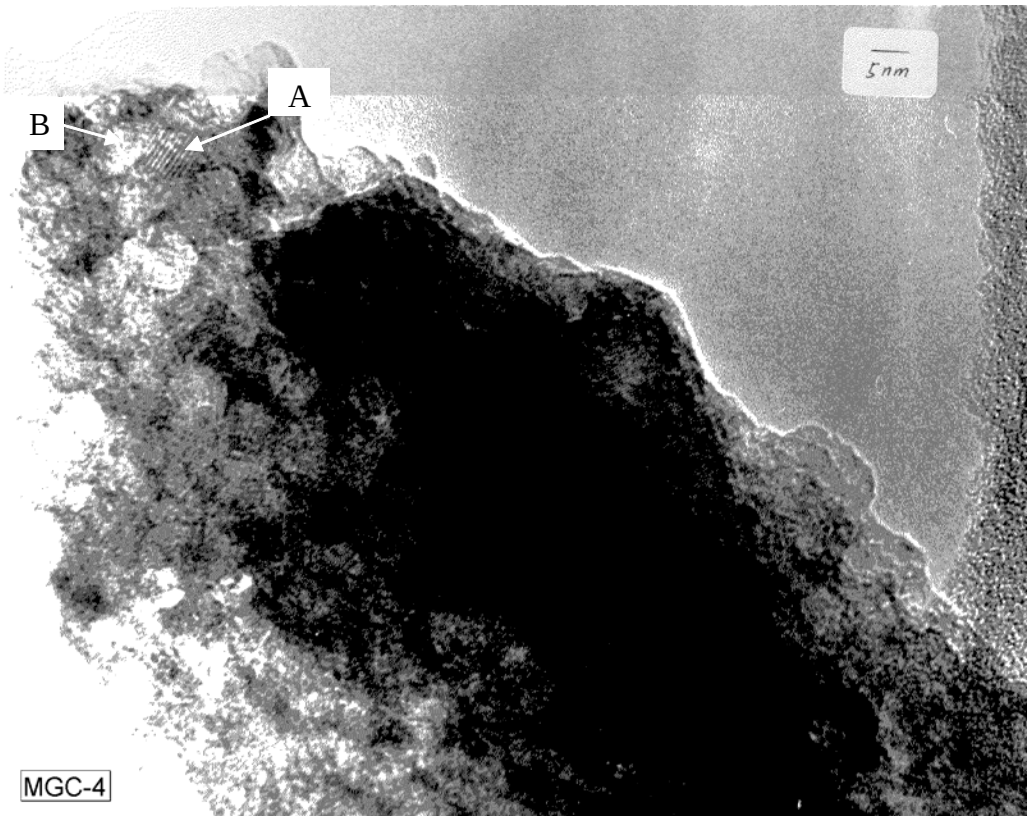

Fig.7 TEM image of the 30 hour ball milled material Mg50%+Ni50%. The material shows the composite structure. The nanoscale grains (A) are surrounded by the amorphous inter grain region (B)

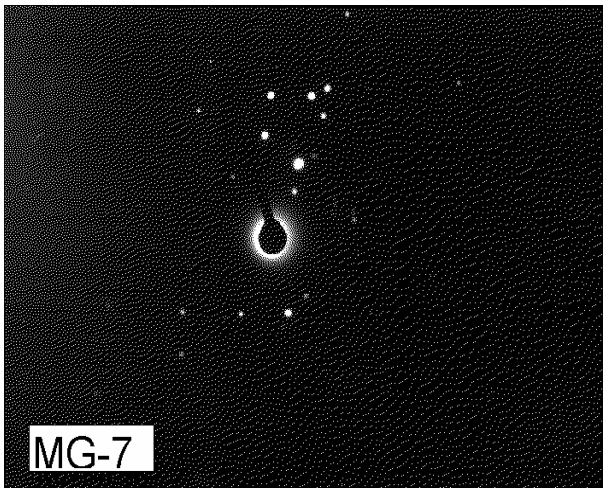

Fig. 8 The electron diffraction pattern of the area A in Fig.1 shows that magnesium is in nano-crystalline state. XRD indicates that the average grain size of magnesium is about 13 nm.

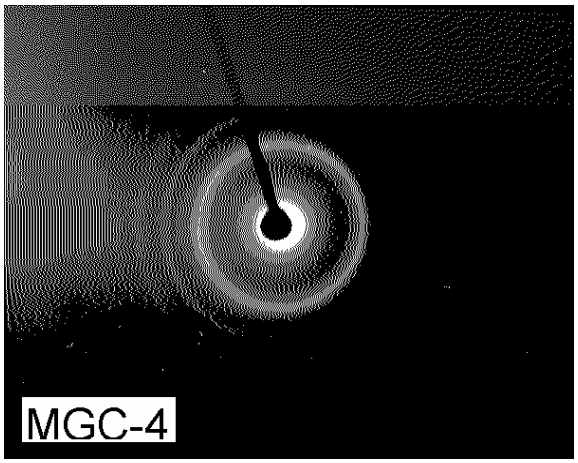

Fig. 9 The electron diffraction pattern of the area B in Fig.1 shows that the nickel is in amorphous state

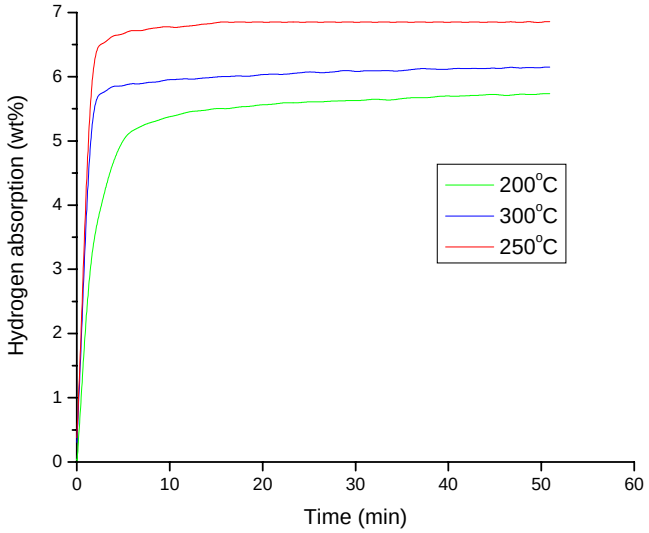

Fig. 10 Hydrogen absorption of the amorphous/nanostructured composite Mg50%-Ni50% materials

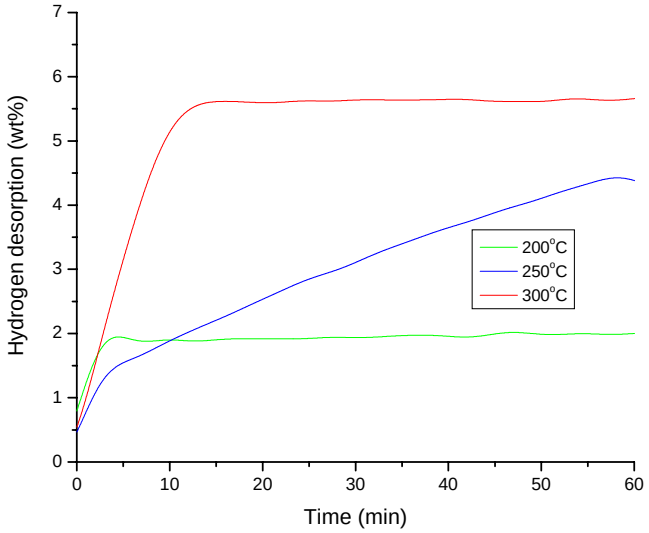

Fig. 11 Hydrogen desorption of the amorphous/nanostructured composite Mg50%-Ni50% materials

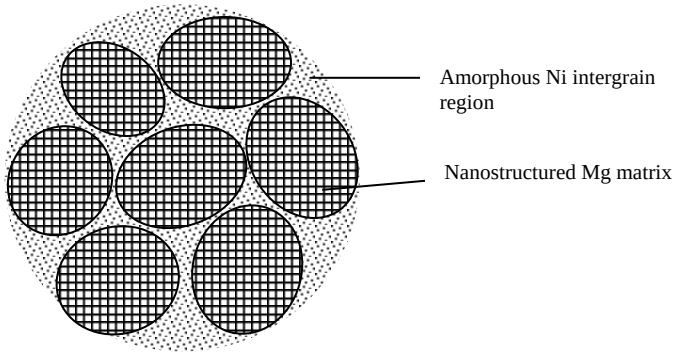

Fig.12 The illustration of the composite structure of Mg-Ni nanostructured/amorphous material

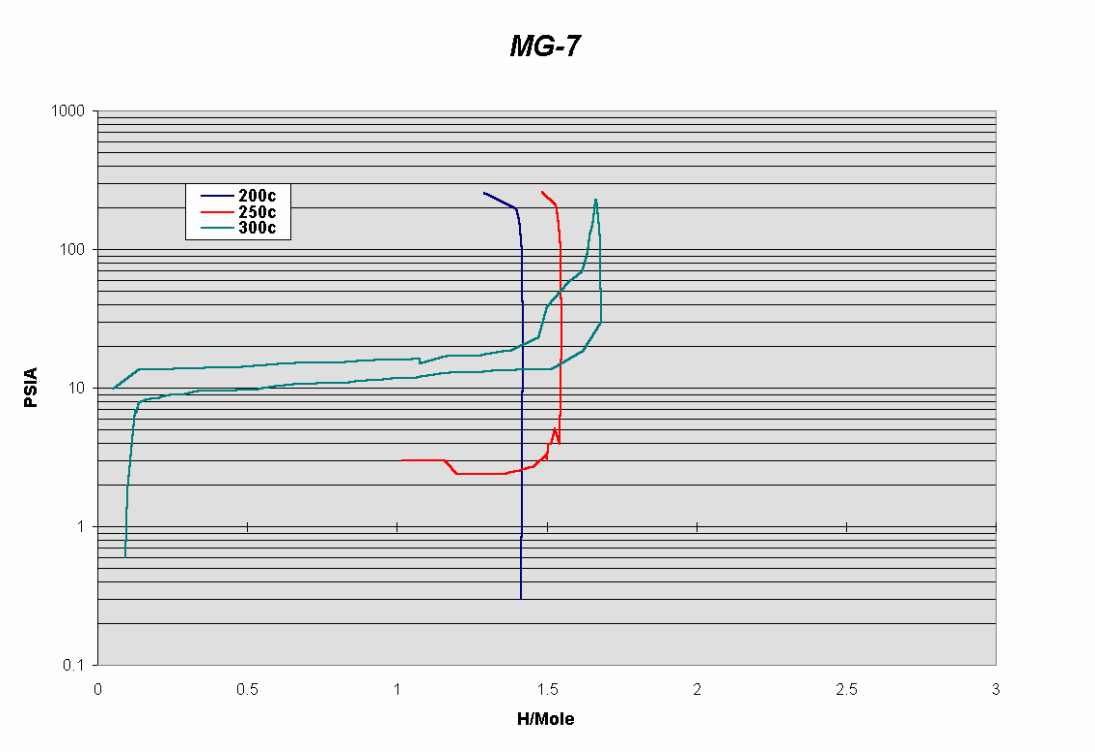

Fig.13 The pressure-composition-isotherm of the nano/amorphous composite material Mg 50wt% - Ni 50wt%

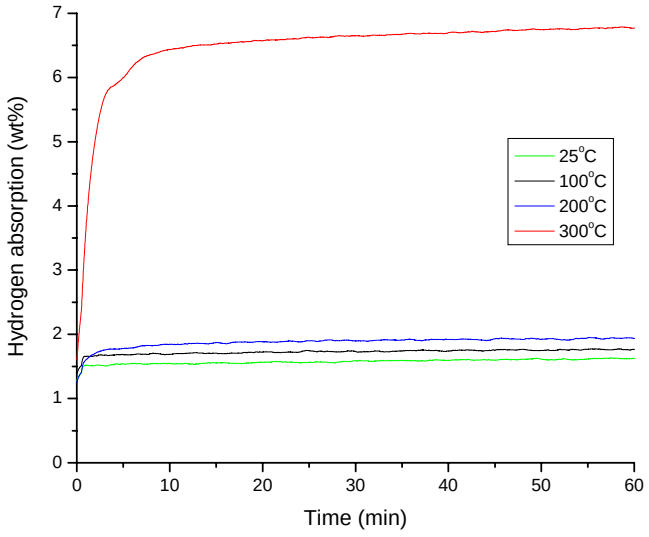

Fig. 14 Hydrogen absorption of the nano/amorphous composite material Mg80%-Ni15%-La 5%

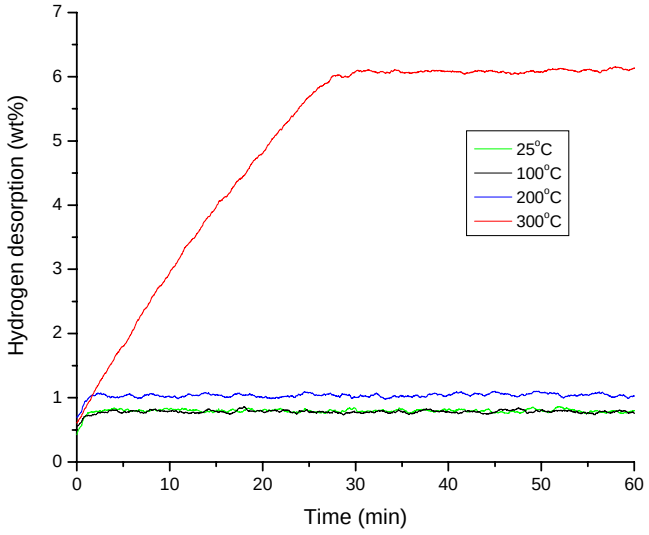

Fig. 15 Hydrogen desorption of the nano/amorphous composite material Mg 80%-Ni15%-La 5%

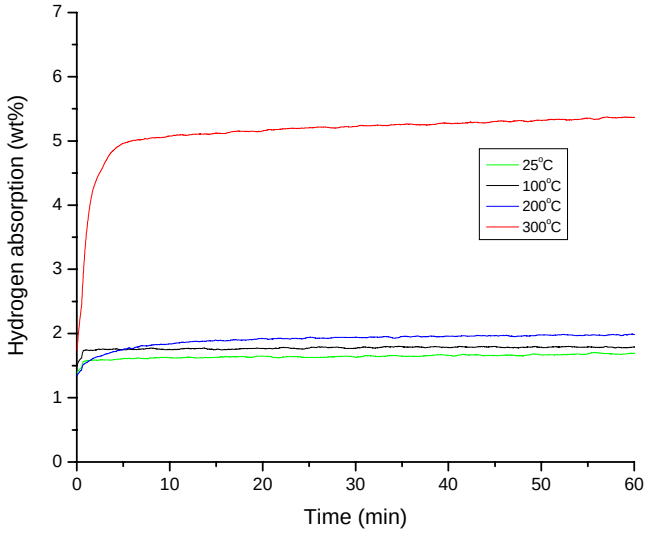

Fig.16 Hydrogen absorption properties of the nano/amorphous composite material Mg70%-Ni20%-La10%

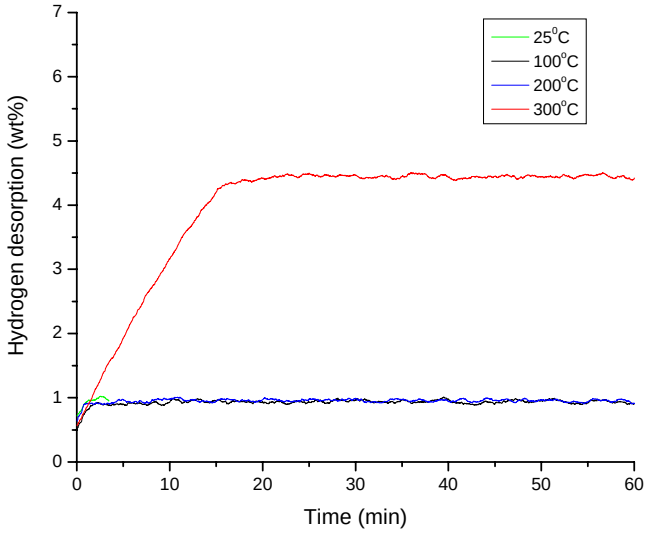

Fig. 17 Hydrogen desorption properties of the nano/amorphous composite material Mg70%-Ni20%-La10%

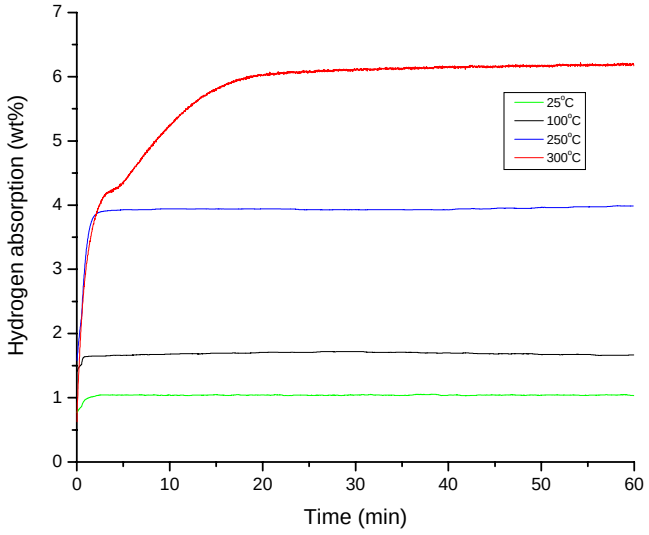

Fig. 18 Hydrogen absorption properties of the nano/amorphous composite material Mg60%-Ni30%-La10%

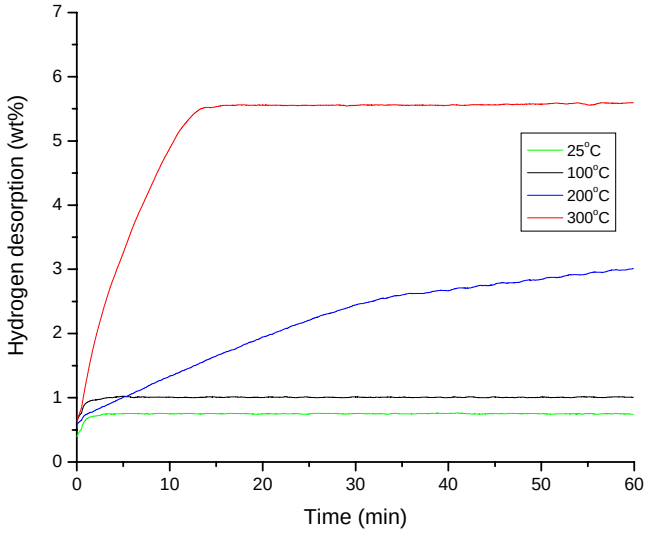

Fig. 19 Hydrogen desorption properties of the nano/amorphous composite material Mg60%-Ni30%-La10%

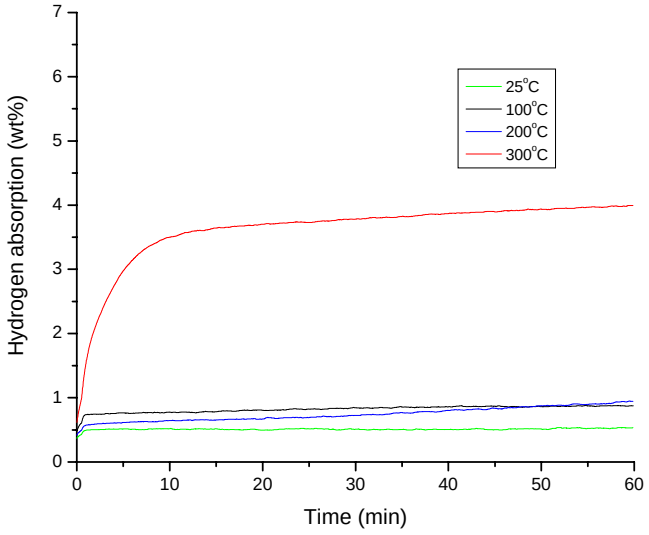

Fig. 20 Hydrogen absorption properties of the nano/amorphous composite material Mg60%-Ni30%-Ce10%

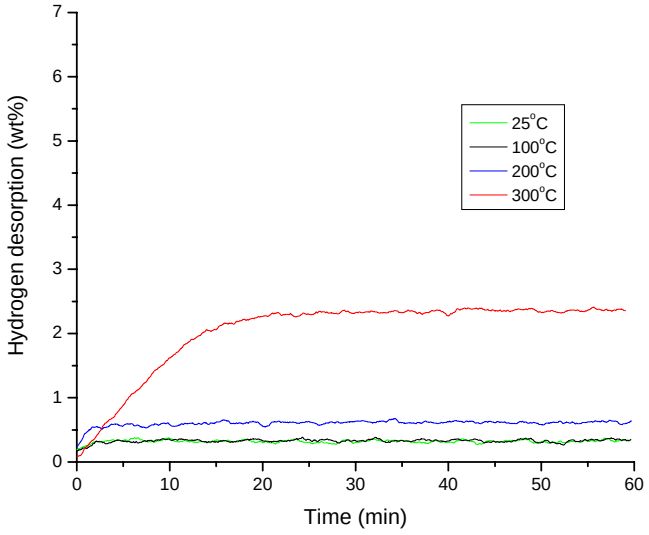

Fig. 21 Hydrogen desorption properties of the nano/amorphous composite material Mg60%-Ni30%-Ce10%

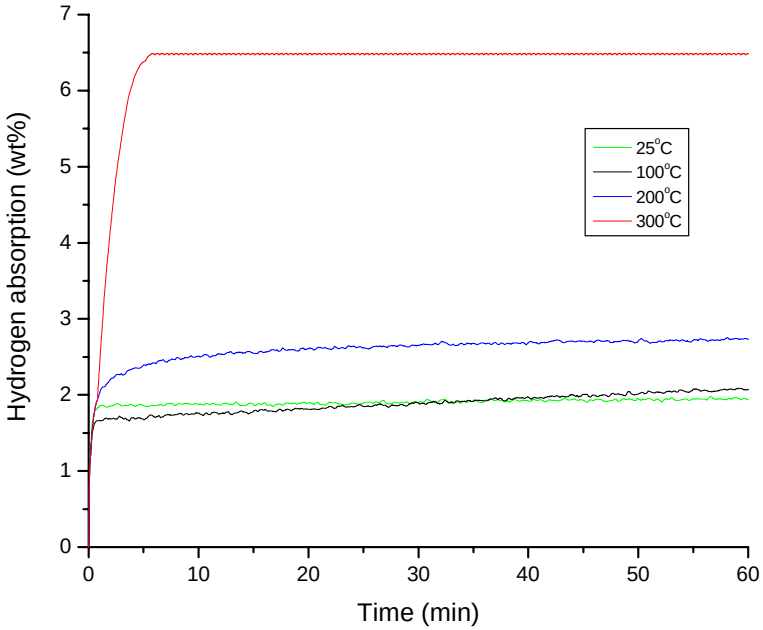

Fig. 22 Hydrogen absorption properties of the material Mg80%-$LaNi_5$ 20%

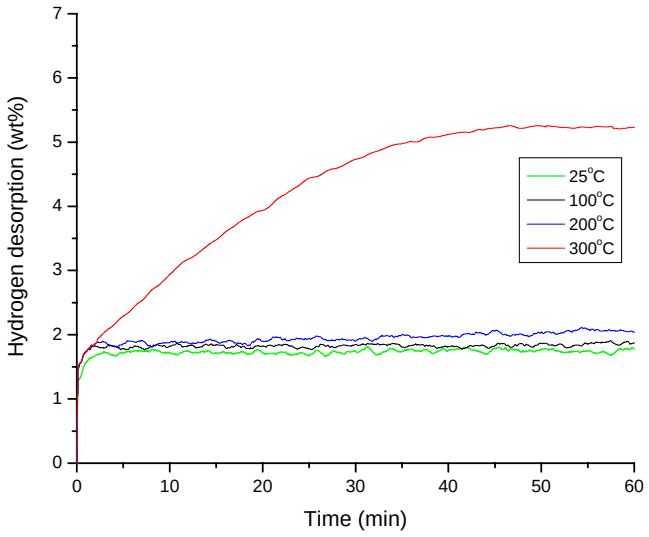

Fig. 23 Hydrogen desorption properties of the material Mg80%-$LaNi_5$ 20%

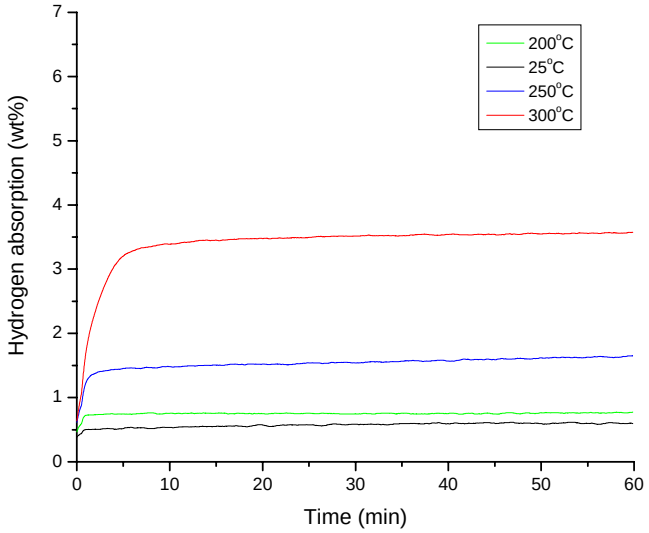

Fig. 24 Hydrogen absorption properties of the material Mg60%-$LaNi_5$ 40%

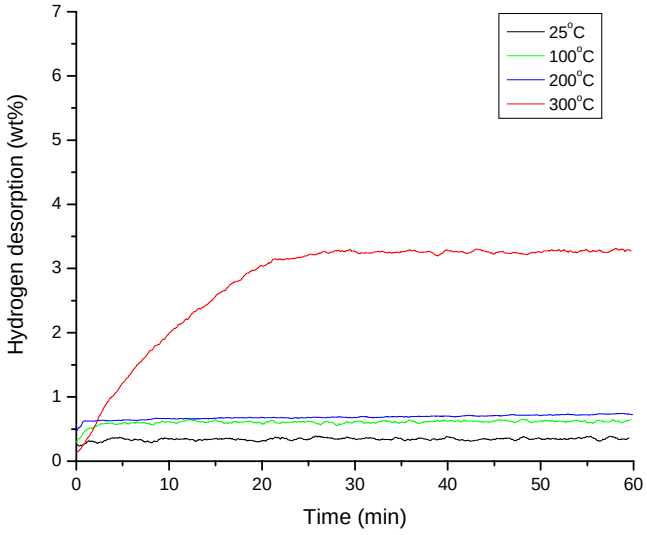

Fig. 25 Hydrogen desorption properties of the material Mg60%-$LaNi_5$ 40%

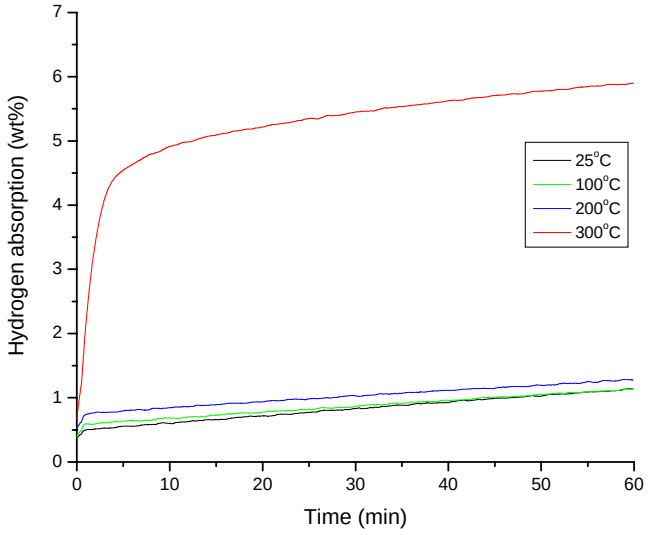

Fig. 26 Hydrogen absorption properties of the material Mg75%-$LaNi_5$ 25%

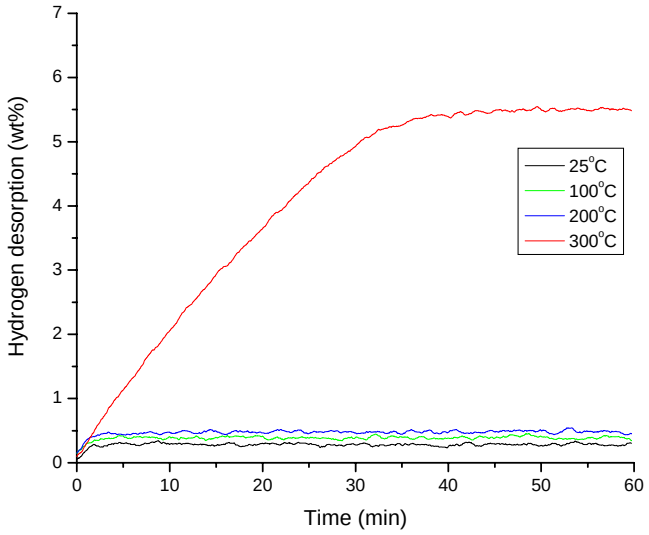

Fig. 27 Hydrogen desorption properties of the material Mg75%-$LaNi_5$ 25%

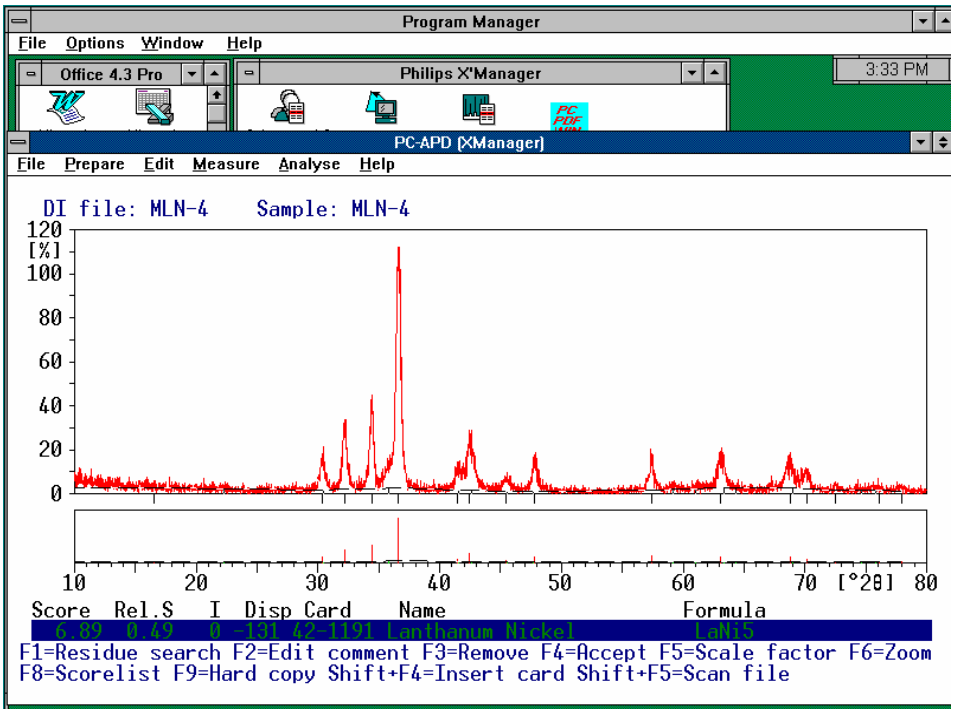

Fig.28 XRD spectrum of the material Mg80%-$LaNi_5$20%

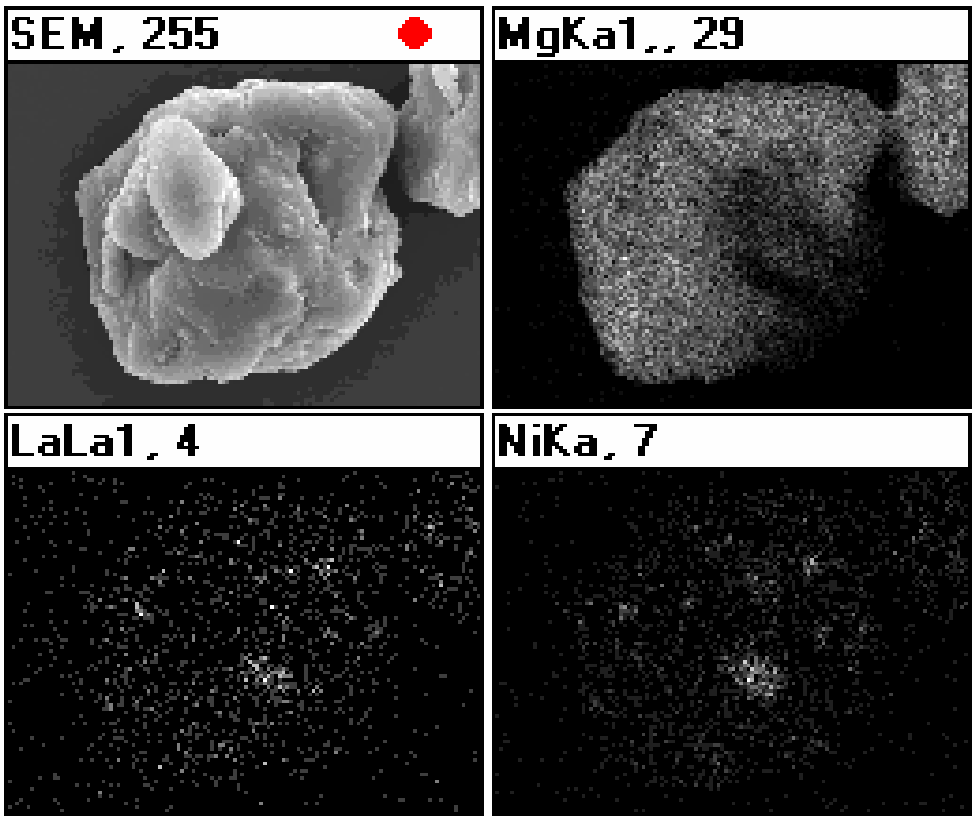

Particle morpholo	Mg map
La map	Ni map

Fig.29 EDX maps of the elements Mg, Ni and La in the nanostructured material Mg-20% $LaNi_5$

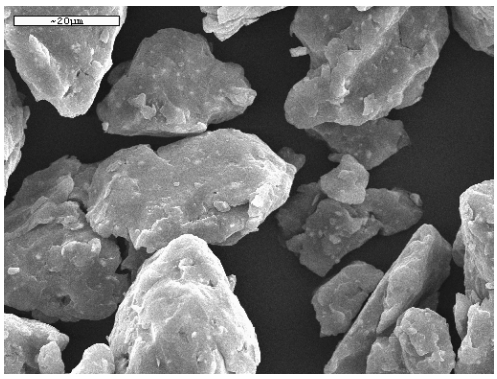

Fig.30 SEM image of the unhydrided material Mg-20% $LaNi_5$ (X1500)

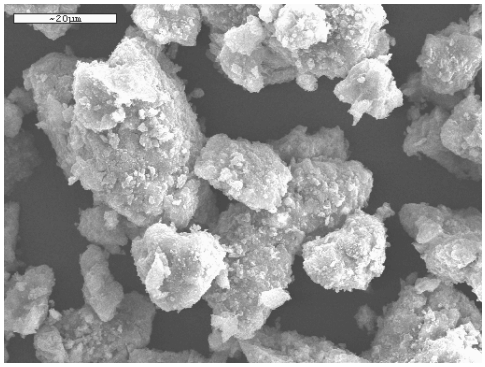

Fig.31 SEM image of the hydrided material Mg-20% $LaNi_5$ (X1500)

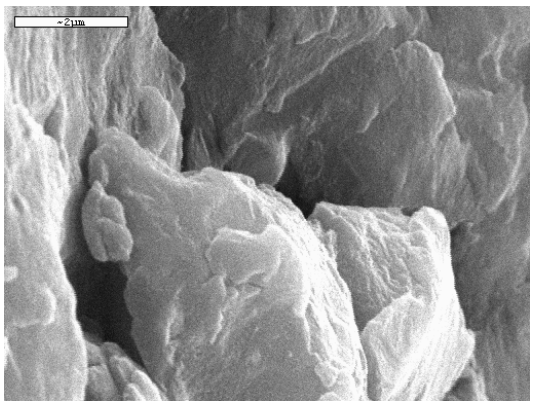

Fig.32 SEM image of the unhydrided material Mg-20% $LaNi_5$. large particles with the smooth surface (X 15000)

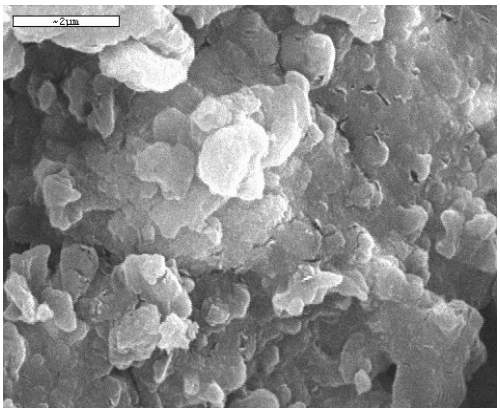

Fig.33 SEM image of the hydrided Mg-20% $LaNi_5$. Smaller particles with cracks (X15000)